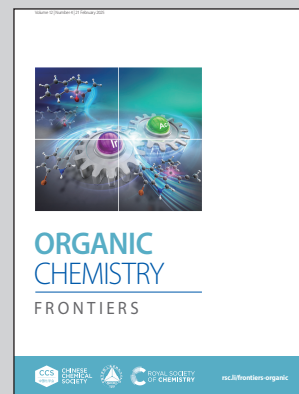


Showcasing research from Professor A. Stephen K. Hashmi's laboratory, Institute of Organic Chemistry, University of Heidelberg, Baden-Württemberg, Germany.

Benzobischalcogeno[3,2-c]quinolines: tuning electronic and structural properties with group 16 elements

Chalcogen-annulated heptacyclic N-heteropolycycles were synthesized. By photophysical and structural analysis, significant properties were observed depending on the annulated chalcogen. It was observed that the heavier the incorporated chalcogen, the better the intermolecular overlap between the molecular layers.

As featured in:



See A. Stephen K. Hashmi *et al.*, *Org. Chem. Front.*, 2025, 12, 1099.

Registered charity number: 207890



CHINESE  
CHEMICAL  
SOCIETY



ROYAL SOCIETY  
OF CHEMISTRY

[rsc.li/frontiers-organic](https://rsc.li/frontiers-organic)

## RESEARCH ARTICLE

View Article Online  
View Journal | View IssueCite this: *Org. Chem. Front.*, 2025, 12, 1099

# Benzobischalcogeno[3,2-*c*]quinolines: tuning electronic and structural properties with group 16 elements†

 Christopher Hübler,<sup>†</sup> Martin C. Dietl,<sup>‡</sup> Matthias Scherr,<sup>‡</sup> Emma Butigan,<sup>a</sup> Robin Heckershoff,<sup>a</sup> Eric F. Lopes,<sup>‡</sup> Justin Kahle,<sup>‡</sup> Petra Krämer,<sup>a</sup> Frank Rominger,<sup>a</sup> Matthias Rudolph<sup>a</sup> and A. Stephen K. Hashmi<sup>‡</sup>\*<sup>a,b</sup>

Chalcogen-substituted  $\pi$ -extended indolocarbazoles were synthesized through a nucleophilic cyclization of tethered diynes with sulfur, selenium or tellurium sources, followed by a Pictet–Spengler reaction. These combined synthetic strategies enabled the facile access to heptacyclic  $\pi$ -extended molecules, offering a broad modularity at various stages of the synthesis route. In total, twenty-six novel heptacyclic compounds were synthesized. Their photophysical and structural properties were investigated experimentally as well as theoretically.

Received 15th October 2024,  
Accepted 29th November 2024

DOI: 10.1039/d4qo01921k

rsc.li/frontiers-organic

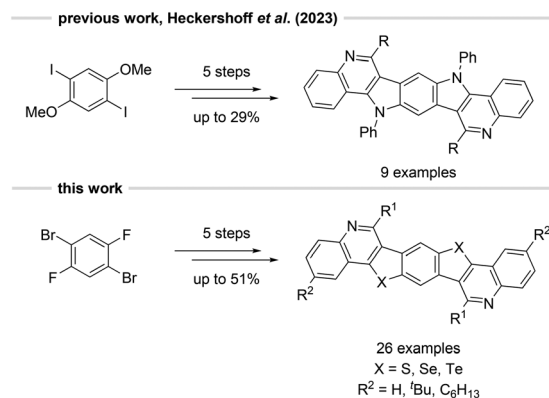
## Introduction

Over the past 70 years, various synthetic procedures for indolocarbazoles (ICZs) have been developed.<sup>1–6</sup> In 2020, our group presented a gold-catalyzed<sup>7–10</sup> approach towards  $\pi$ -extended benzo[*a*]benzo[6,7]indolo[2,3-*h*]carbazoles (BBICZs).<sup>11</sup> These BBICZs show hole transport mobilities of up to 1 cm<sup>2</sup> V<sup>−1</sup> s<sup>−1</sup> in organic thin-film transistors (TFT).<sup>12</sup> Such  $\pi$ -conjugated N-heteropolycyclic molecules are promising compounds for applications in organic light-emitting diodes (OLEDs),<sup>13–16</sup> organic field-effect transistors (OFETs),<sup>11,12,17–19</sup> or organic photovoltaics (OPV).<sup>20,21</sup> By isosteric replacements of CH-units by nitrogen atoms, the electronic properties of these molecules can be modified, for example in azaacenes,<sup>22,23</sup> tetraazaperopyrenes,<sup>24</sup> or dipyrrolopyrazines.<sup>25,26</sup> We applied this technique to our previously synthesized BBICZs for the synthesis of benzobispyrrolo[3,2-*c*]quinolines (BBPQs) via a bidirectional Pictet–Spengler reaction.<sup>27</sup>

Now we envisioned the replacement of the indole NH groups of BBPQs with chalcogen atoms to obtain benzobischalcogeno[3,2-*c*]quinolines (BBCQs) (Scheme 1), which we report here. Thiophene-fused  $\pi$ -conjugated molecules show

greater stability against degradation, making them appealing for the fabrication of electronic and optical devices.<sup>28</sup> Moreover, the incorporation of heavy chalcogen atoms is associated with an enhanced orbital overlap, therefore increasing charge mobility, particularly in organic photovoltaics.<sup>29–32</sup> In addition, the synthesis of the central benzodichalcogenophen-core is achieved through a short sequence.

Prior to its application in the syntheses of BBPQs, the use of the Pictet–Spengler reaction in materials science was scarce with only a few examples documented.<sup>33–35</sup> Its original application more than 100 years ago primarily involved the synthesis of alkaloid skeletons, such as tetrahydroisoquinoline derivatives, which depict a pharmacological importance, for



**Scheme 1** Previous Pictet–Spengler-approach towards benzobispyrrolo[3,2-*c*]quinolines<sup>27</sup> and our procedure to obtain the chalcogenated congeners. Overall yields are presented.

<sup>a</sup>Organisch-Chemisches Institut (OCI), Heidelberg University, Im Neuenheimer Feld 270, 69120 Heidelberg, Germany. E-mail: hashmi@hashmi.de

<sup>b</sup>Chemistry Department, Faculty of Science, King Abdulaziz University, Jeddah, 21589, Saudi Arabia

†Electronic supplementary information (ESI) available: Experimental procedures, analytical data and spectra. CCDC 2380037–2380046. For ESI and crystallographic data in CIF or other electronic format see DOI: <https://doi.org/10.1039/d4qo01921k>

‡These authors contributed equally to this work.



instance in the preparation of antihypertensive drugs, hence highlighting it as one of the fundamental reactions in natural product and pharmaceutical synthesis.<sup>36–39</sup>

## Results and discussion

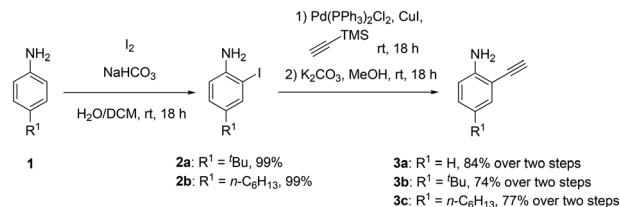
### Syntheses of BBCQs

To synthesize the target heptacyclic BBCQs, we envisioned a convergent modular strategy which has proven successful in our previous work, allowing a quick and variable synthesis by combining building blocks (Scheme 2).<sup>11</sup> Firstly, building blocks **A** and **B** were combined in a Sonogashira coupling, introducing variability by the utilization of different alkyne components. Subsequently, the obtained diyne moieties underwent cyclization using nucleophilic chalcogen sources **C**. Finally, a Pictet–Spengler reaction with various aldehydes **D** was conducted to access BBCQs. This approach results in three reactions where a modular procedure is possible, facilitating the incorporation of various substituents, enabling the synthesis of a wide range of potentially semiconducting molecules.

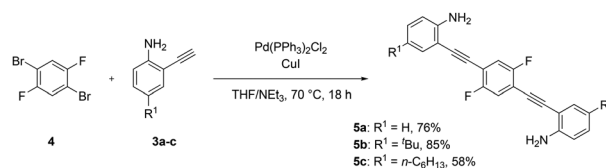
The central precursor for the target compounds, 1,4-dibromo-2,5-difluorobenzene **4** (building block **A** in Scheme 2) serves as a cheap and commercially available starting material.

The synthesis of building block **B** consists of an *ortho*-iodination of *para*-alkylated (*tert*-butyl and *n*-hexyl) anilines **1** through a modified literature procedure according to Flynn *et al.*, resulting in **2a** and **2b** in quantitative yield.<sup>40</sup> The choice of alkyl substituents was made to avoid poor solubilities of the addressed large planar systems. Subsequently, these compounds underwent a Sonogashira coupling with the non-alkylated, commercially available, 2-iodoaniline, followed by a deprotection. The resulting 4-alkylated or unsubstituted *ortho*-ethynyl-anilines **3a–c** were obtained in high yields ranging from 74 to 84% over two steps (Scheme 3).

By reacting building block **A** and **B** *via* a Sonogashira reaction, diynes **5a–c** were synthesized in good yields of 58 to 85% (Scheme 4). These compounds might serve as promising blue emitters based on their optical properties, with quantum



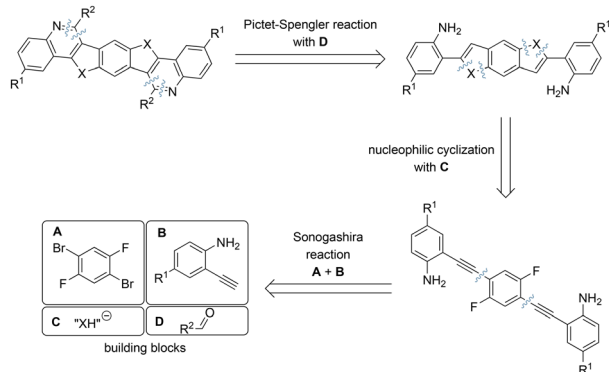
**Scheme 3** Synthesis of building blocks **B**, impersonated by compounds **3a–c**.



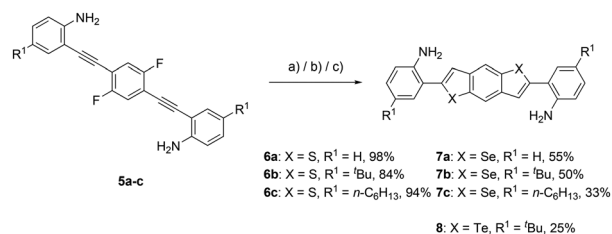
**Scheme 4** Sonogashira reaction of building blocks **A** and **B**.

yields of up to 74% and emission wavelengths ranging from 450 to 469 nm, suggesting potential applications in organic devices. For **5a** and **5b**, crystals suitable for single crystal X-ray structure analysis were obtained (see the ESI†).

In the next step, the diynes were subjected to bidirectional nucleophilic substitution and subsequent hydrochalcogenation with building block **C** (Scheme 5). The use of *N*-methyl-2-pyrrolidone (NMP) as a high boiling solvent was essential for the successful two-fold reaction. This choice of an aprotic polar solvent is in agreement with known procedures for synthesising benzodichalcogenophenes.<sup>41,42</sup> Another notable aspect within this step is the direct precipitation of the products, simplifying the work up, only decantation or filtration followed by washing are necessary. The synthesis of the thiophene ring of the benzodithiophenes **6a–c** proceeded smoothly under open flask conditions when using sodium sulfide, yielding the desired products in excellent yields of up to 98%. For generation of the selenophene subunit, the reactive hydrogen selenide was prepared *in situ* by using LiBEt<sub>3</sub>H and elemental selenium. After the subsequent addition of the reactant and overnight heating, the benzodiselenophenes **7a–c** were formed in moderate yields of up to 55%. The benzoditellurophene **8** was prepared following a similar procedure as for selenium in



**Scheme 2** Modular building block principle for the synthesis of BBCQs.



**Scheme 5** Bidirectional nucleophilic hydrochalcogenation. a) (**6a–c**): Na<sub>2</sub>S, Cul, NMP, 180 °C, overnight; b) (**7a–c**): LiBEt<sub>3</sub>H, Se, THF/NMP, 180 °C, overnight; c) (**8**): LiBEt<sub>3</sub>H, Te, THF/NMP, 180 °C, overnight.



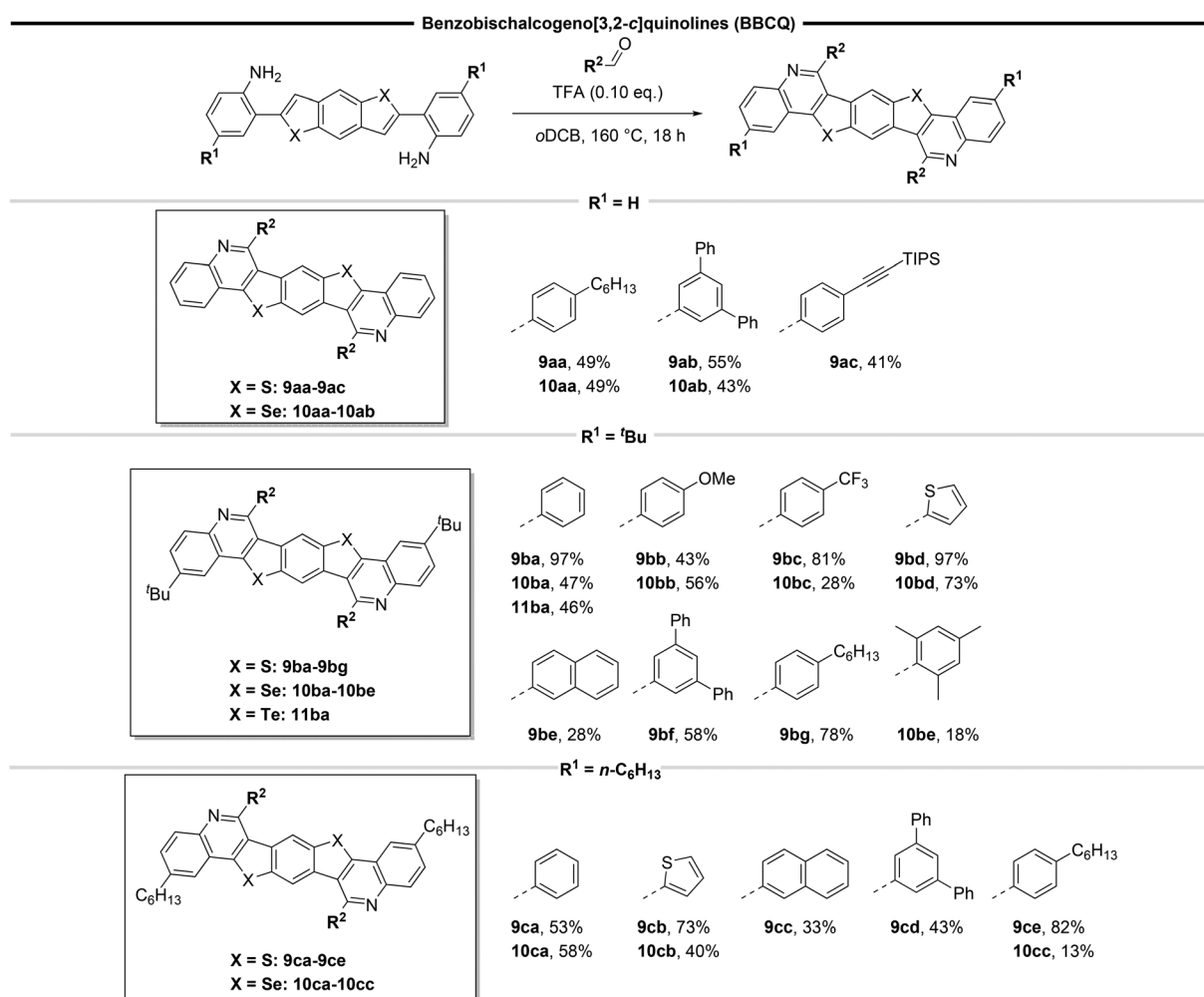
a moderate yield of 25%. Additionally, single crystals suitable for single crystal X-ray structure analysis were obtained for **8** (see the ESI†). Only the *tert*-butyl-substituted derivative of this benzoditellurophene was synthesized, demonstrating the ability to prepare the telluracycles.

To obtain the target molecules, compounds **6–8** were subjected to a Pictet–Spengler reaction, employing various aldehydes (building block **D**) to yield BBCQs **9–11** (Scheme 6). Initially, the known procedure for synthesizing BBPQs was used.<sup>27</sup> However, these reaction conditions were optimized for the activated nucleophilic C3-site<sup>43</sup> of the indole moieties. When applied to our system, no reaction occurred. To our delight, this issue was overcome by applying elevated temperatures of 160 °C in *ortho*-dichlorobenzene (*o*DCB) as solvent. Additionally, trifluoroacetic acid (TFA) was employed instead of *para*-toluenesulfonic acid as a more acidic catalyst to ensure a complete conversion.

It is noteworthy that in the case of the non-alkylated bis-chalcogenophenes **6a** and **7a**, only substituents exhibiting high solubility (**9aa**, **9ac** and **10aa**) or interference with the  $\pi$ -stacking (**9ab**, **10ab**) could be introduced. When aldehydes

lacking these properties were used, due to low solubility the product could not be fully characterized. Products **9aa–9ac** and **10aa–10ab** were obtained in satisfactory yields of 41 to 55%. Examining the *tert*-butyl substituted examples **9b**, **10b** and **11b**, a wide range of target molecules was obtained. Multiple substituents with various properties, including electron-neutral (**9ba**, **9bf**, **9bg**, **10ba**, **10be**, **11ba**), electron-donating (**9bb**, **10bb**), electron-withdrawing (**9bc**, **10bc**), heterocyclic (**9bd**, **10bd**) or polycyclic (**9be**) examples were introduced successfully thanks to the *tert*-butyl group inducing solubility and therefore simplifying the workup process. However, the scope is limited to the use of aryl aldehydes, since aliphatic aldehydes undergo prior aldol condensation under our conditions, resulting in multiple side products (depending on the grade of oligomerization of the aldehyde) that cannot be separated due to similar polarities and solubilities. This effect was also observed in the synthesis of smaller systems under milder conditions.<sup>44</sup> Additionally, no product formation is observed when using 2,2-disubstituted alkyl aldehydes.

Usually, for thiophenes the best yields are obtained, followed by selenophenes and tellurophenes. The yield of benzo-



**Scheme 6** Synthesis of BBCQs **9–11**.



bisthieno[3,2-*c*]quinolines **9b** is significantly higher compared to the selenium-substituted counterparts **10b** in most instances. Moreover, aldehydes bearing sterically demanding groups **R**<sup>2</sup> could not be implemented. In the case of benzobis-telluro[3,2-*c*]quinoline **11ba**, a successful conversion was accomplished with a yield of 46%. While in theory, additional examples could be obtained, only **11ba** was synthesized for the sake of illustrating the reaction principle.

Finally, *n*-hexyl substituted BBCQs **9c** and **10c** were synthesized in low to good yields of 13–82%. It is noteworthy that, apart from the presented substituents **R**<sup>2</sup>, other aldehydes can be used for the synthesis of **9b**, **10b** and **11b**.

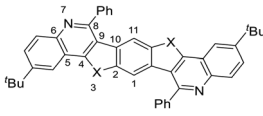
### Structural properties

For numerous BBCQs, specifically **9aa**, **9ba**, **9bc**, **10ba**, **10be**, **10cc** and **11ba**, single crystal X-ray structure analyses were conducted. In the following paragraph, the solid-state molecular structures of **9ba**, **10ba** and **11ba** will be discussed (Fig. 1; for all obtained molecular structures, see the ESI†).

All three compounds bear a *tert*-butyl substituent at the **R**<sup>1</sup> position, while the chalcogen units vary between sulfur, selenium and tellurium. The triclinic *P* $\bar{1}$  space group is present in all examples, with one molecule per unit cell, and are located on crystallographic inversion centres. The central conjugated  $\pi$ -system remains fully planar in each instance. In the subsequent section, selected bond lengths, bond angles and packing motifs will be discussed by direct comparison of **9ba**, **10ba** and **11ba**, as the chalcogen atom represents the only difference among them (Table 1).

Significant disparities are observed in the lengths of the C2–X3 bond and the C4–X3 bond, elongating by approximately 0.13 Å when comparing **10ba** with **9ba**. In the case of tellurium, this elongation increases to about 0.20–0.22 Å in comparison to the selenium-substituted congener. This observation probably results from the increasing van der Waals radii in group 16. Consequently, the bond angles C2–X3–C4 decrease, and C2–C10–C9 increase with higher atomic number. All other bond lengths and angles do not differ sig-

**Table 1** Selected bond distances (Å) and angles (°) of **9ba**, **10ba** and **11ba**



	X = S ( <b>9ba</b> )	X = Se ( <b>10ba</b> )	X = Te ( <b>11ba</b> )
<i>d</i> (X3–C2)	1.743(2) Å	1.873(5) Å	2.079(4) Å
<i>d</i> (X3–C4)	1.736(2) Å	1.868(5) Å	2.089(4) Å
$\angle$ (C2–X3–C4)	91.14(9)°	86.4(2)°	81.33(17)°
$\angle$ (C2–C10–C9)	111.00(17)°	112.9(4)°	115.7(4)°

nificantly from each other. Despite being substituted with a bulky *tert*-butyl group which would typically hinder an ordered orientation, all examples are stacked in a planar fashion in the packing motifs. Furthermore, strong  $\pi$ – $\pi$  interactions are observed in all crystal structures with intermolecular distances between molecule planes of 3.827 Å for **9ba**, 4.044 Å for **10ba** and 4.111 Å for **11ba**. This trend is also likely attributed to the increasing van der Waals radii of the chalcogens.

Another interesting observation is the dependence of the incorporated substituent **R**<sup>2</sup> on the packing motif (Fig. 2).

When 4-(trifluoromethyl)benzaldehyde is used, the packing motif of the BBCQ changes drastically, from a layer structure to a herringbone-type motif, with a herringbone angle of 79°. Therefore, the molecular packing motif can be influenced by the choice of building block **D** (Scheme 2), emphasizing the importance of modularity of the synthetic approach towards BBCQs.

### Optoelectronic properties

Precursors **5–8** and BBCQs **9–11** were studied by UV-Vis and fluorescence spectroscopy in DCM (Fig. 3 and Table 2). Compounds **5a–c** exhibit comparable absorption and emission

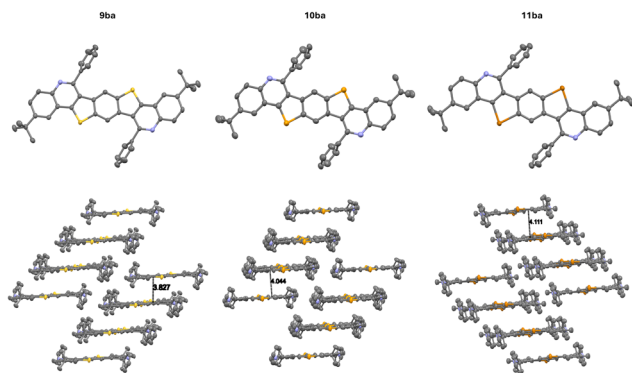


**Fig. 1** Solid state molecular structures (top) and packing motifs (bottom) of **9ba** (CCDC 2380041), **10ba** (CCDC 2380043) and **11ba** (CCDC 2380046).† The thermal ellipsoids are set at a 50% probability level and hydrogen atoms are omitted for clarity.

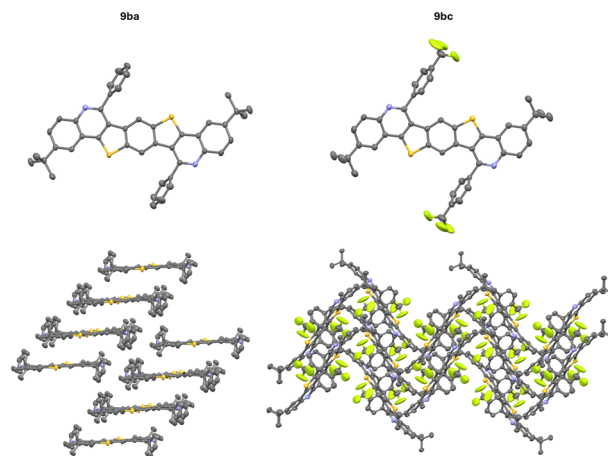


**Fig. 2** Comparison of the solid state molecular structures (top) and packing motifs (bottom) of **9ba** (CCDC 2380041) and **9bc** (CCDC 2380042).† The thermal ellipsoids are set at a 50% probability level and hydrogen atoms are omitted for clarity.



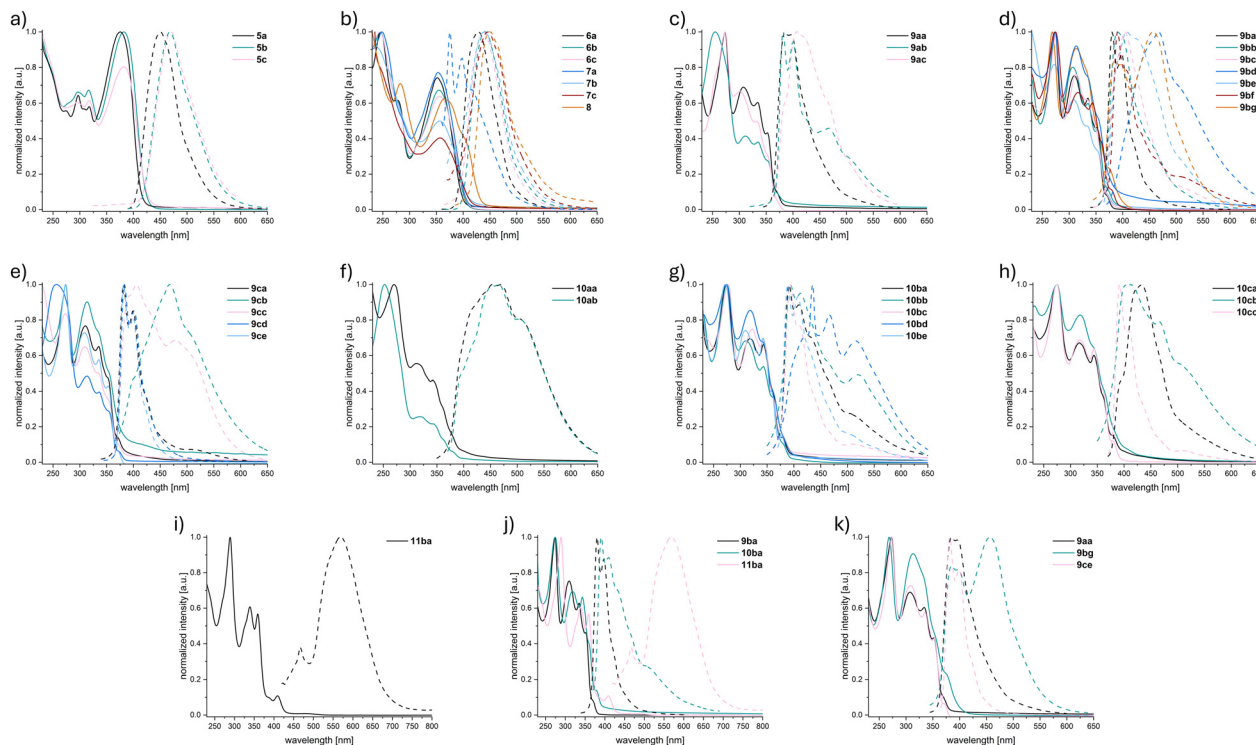


**Fig. 3** Normalized absorption (solid line) and emission (dashed line) spectra in DCM of a) 5a–c; b) 6–8; c) 9aa–9ac; d) 9ba–9bg; e) 9ca–9ce; f) 10aa–10ab; g) 10ba–10be; h) 10ca–10cc; i) 11ba; j) 9ba, 10ba and 11ba; k) 9aa, 9bg and 9ce.

properties, with absorption maxima ranging from 376 to 382 nm and emission maxima of 450 to 469 nm, respectively. These compounds show high quantum yields of 61–74%. For 6a–c, 7a–c and 8, a trend in quantum yields is observed. Quantum yields for sulfur-containing compounds range from 16 to 17% but decrease significantly for selenium-containing counterparts to 2–3% and drop below 1% for the respective ditellurophene. Benzodichalcogenophen precursors 6 and 7 exhibit similar values for the absorption maxima of 352 to 357 nm, while tellurophene 8, shows an absorption maximum at 404 nm. Emission maxima range from 376 to 450 nm, with optical bandgaps calculated based on the absorption onset ranging from 2.87 to 3.10 eV.

Examining BBCQs 9, 10 and 11, multiple trends emerge. Firstly, minor influence of different substituents  $R^2$  is observed. Negligible differences in absorption maxima are noted when comparing unsubstituted sulfur-containing examples 9a, as well as *tert*-butyl- or *n*-hexyl-substituted examples 9b and 9c. However, for 9bd and 9cb ( $R^2 = 2$ -thiophene), a remarkable blue shift of the absorption maximum is observed. Comparison of thiophen- and selenophen-annulated BBCQs indicates, that the absorption maxima are redshifted with heavier chalcogens. This trend is also reflected in the optical bandgaps, with slightly smaller values of 3.06–3.21 eV for examples 10, compared to 3.07–3.38 eV for examples 9. The direct influence of the chalcogen used on the optical bandgap is apparent when comparing the absorption spectra of 9ba, 10ba and 11ba, all having the same substituents  $R^1$  and  $R^2$ .

The general substitution of alkyl substituents  $R^1$  has a remarkable impact on the photophysical properties of BBCQs. Comparing 9aa, 9bg and 9ce reveals a redshift of 22–27 nm for the absorption maxima. However, discrepancies between *tert*-butyl and *n*-hexyl substituents are marginal. These alkyl substituents  $R^1$  have a higher impact on the fluorescence spectra than the implemented aldehydes  $R^2$  when comparing 9a and 10a ( $R^1 = H$ ) to their alkyl substituted counterparts. In this case, emission maxima range from 383 to 450 nm, resulting in Stokes shifts of 2139–4163  $\text{cm}^{-1}$ , except for *n*-hexyl substituted 10ca and 10cb, which exhibit emission maxima of 408–433 nm, resulting in Stokes shifts of 2963–3152  $\text{cm}^{-1}$ . Moreover, compounds 9bd, 9cb, 10bd and 10cb, all with  $R^2$  as 2-thiophen, show high emission maxima (408–468 nm) and large Stokes shifts (2963–6801  $\text{cm}^{-1}$ ). Fluorescence quantum yields (QY) are in the low range of 1–8% for sulfur-substituted compounds 9. For selenium- and tellurium-substituted counterparts 10 and 11, the QY barely reaches the 1%-mark. This observation is most likely contributed to the heavy-atom-effect,<sup>45</sup> which is induced by the presence of selenium and tellurium atoms.

### Quantum chemical calculations

For the frontier orbital energies of 9–11, DFT calculations were performed using Orca 5.0.3.<sup>46</sup> The B3LYP/G functional and the def2-TZVP basis set were employed for the calculations (Table 2, see the ESI for more details<sup>†</sup>).<sup>47–50</sup> For the sulfur-substituted compounds 9, the HOMO-energies are located



Table 2 Photophysical properties of 5–11 measured in DCM

Compound	$\lambda_{\text{max,abs}}^a$ [nm]	$\lambda_{\text{max,em}}^b$ [nm]	Stokes shift [cm <sup>-1</sup> ]	$\lambda_{\text{onset,abs}}$ [nm]	$E_{\text{g(opt)}}^c$ [eV]	QY <sup>d</sup> [%]	HOMO <sup>e</sup> [eV]	LUMO <sup>e</sup> [eV]	$E_{\text{g(calc)}}^f$ [eV]
5a	376	450	4374	413	3.00	66	—	—	—
5b	382	468	4810	423	2.93	74	—	—	—
5c	382	469	4856	427	2.90	61	—	—	—
6a	352	429	5099	400	3.10	16	—	—	—
6b	355	441	5493	403	3.07	16	—	—	—
6c	356	438	5259	407	3.05	17	—	—	—
7a	353	376	1733	406	3.05	2	—	—	—
7b	356	439	5311	416	2.98	2	—	—	—
7c	357	446	5590	417	2.98	3	—	—	—
8	404	450	2530	432	2.87	<1	—	—	—
9aa	353	383	2219	367	3.38	4	-5.88	-2.00	3.88
9ab	354	383	2139	371	3.34	3	-5.99	-2.11	3.88
9ac	354	407	3679	371	3.34	2	-6.02	-2.17	3.85
9ba	371	380	638	382	3.24	5	-5.85	-1.97	3.88
9bb	372	390	1241	395	3.14	4	-5.91	-2.04	3.86
9bc	370	386	1120	403	3.07	4	-6.00	-2.14	3.86
9bd	356	466	6631	380	3.26	4	-5.91	-2.03	3.87
9be	373	405	2118	391	3.17	1	-5.84	-1.98	3.87
9bf	377	390	884	395	3.14	3	-5.77	-2.14	3.63
9bg	375	385	693	401	3.09	4	-5.93	-2.05	3.88
9ca	371	382	776	391	3.17	4	-5.92	-2.04	3.88
9cb	355	468	6801	382	3.24	8	-5.96	-2.07	3.89
9cc	375	390	1026	392	3.16	1	-5.92	-2.09	3.83
9cd	373	383	700	387	3.20	2	-5.94	-2.11	3.83
9ce	380	391	740	395	3.14	3	-5.92	-2.07	3.85
10aa	379	450	4163	400	3.10	<1	-5.94	-2.13	3.81
10ab	380	450	4094	405	3.06	<1	-5.92	-2.15	3.77
10ba	380	391	740	397	3.12	1	-5.87	-2.11	3.77
10bb	379	393	940	395	3.14	<1	-5.84	-2.08	3.77
10bc	377	393	1080	402	3.08	<1	-5.93	-2.17	3.76
10bd	364	435	4484	386	3.21	<1	-5.90	-2.14	3.76
10be	378	389	748	394	3.14	1	-5.86	-2.07	3.79
10ca	381	433	3152	403	3.07	1	-5.87	-2.11	3.75
10cb	364	408	2963	391	3.17	<1	-5.89	-2.16	3.73
10cc	381	392	737	395	3.14	1	-5.85	-2.10	3.75
11ba	409	468	3082	430	2.88	<1	-5.66	-2.14	3.52
BBPQ-Ph <sup>g</sup>	364	395	2156	388	3.20	10	-5.62	-1.74	3.88

<sup>a</sup> Maximum of the longest absorption wavelength. <sup>b</sup> Maximum of the shortest emission wavelength. <sup>c</sup> Optical gap estimated from  $\lambda_{\text{onset,abs}}$ .  $E_{\text{g(opt)}} = 1239.8/\lambda_{\text{onset,abs}}$ . <sup>d</sup> Fluorescence quantum yield. <sup>e</sup> Data derived from DFT-calculations. <sup>f</sup> HOMO-LUMO gap. <sup>g</sup> Data from an earlier publication.<sup>27</sup>

between -6.02 and -5.77 eV, while the LUMO-energies range from -2.17 to -1.97 eV, resulting in theoretical band gaps of 3.63–3.89 eV. For the selenium-substituted compounds **10**, the HOMO-energies are located between -5.94 and -5.84 eV, and the LUMO-energies range from -2.17 to -2.07 eV, leading to theoretical band gaps of 3.73–3.85 eV. **11ba** exhibits the smallest theoretical band gap of 3.52 eV with a HOMO-energy of -5.66 eV and a LUMO-energy of -2.14 eV. It is observable that the variation of the band gap among each group of BBCQs is minimal. This can be attributed to the fact that, for all examples **9**–**11**, the HOMO and LUMO are located within the  $\pi$ -conjugated heptacycle (Fig. 4, see the ESI for more details<sup>†</sup>).

Additionally, it becomes apparent that the substituents **R**<sup>1</sup> and **R**<sup>2</sup> only exhibit a marginal electron density in the HOMO and a node in the LUMO, leading to the conclusion that they are not part of the conjugated  $\pi$ -system, which explains the small differences in both the theoretical and optical band gaps. This was also observed for the BBPQs we reported previously.<sup>27</sup> When compared to the optical band gaps, the

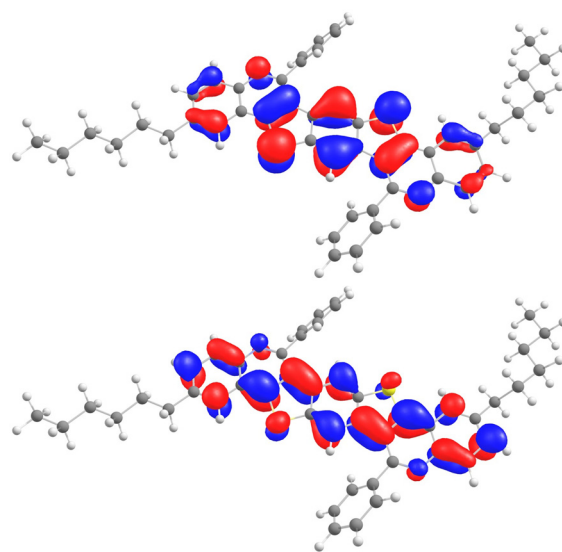
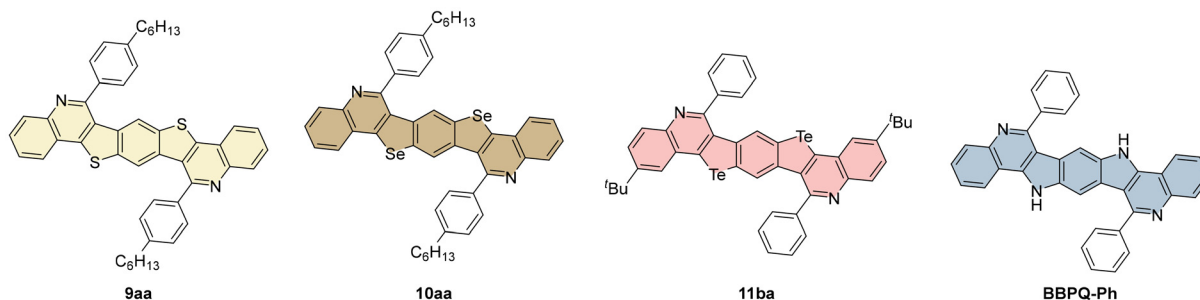


Fig. 4 Calculated frontier molecular orbitals of **9ca**; top: LUMO, bottom: HOMO.





**Fig. 5** BBCQs **9aa**, **10aa**, **11ba** and structurally related **BBPQ-Ph**,<sup>27</sup> which are used to compare the difference in the photophysical properties caused by isosteric replacement of pyrrolo-NH moieties by chalcogen atoms.

theoretical gaps show a consistent discrepancy of 0.49 to 0.79 eV due to the inherent tendency of the calculations to overestimate the LUMO energies.

### Comparison to structurally related analogues

To examine the impact of isosteric replacements of heteroatoms within the 5-membered ring of the heptacycles, **9aa**, **10aa** and **11ba** were compared to structurally related **BBPQ-Ph**, previously discussed in an earlier publication (Fig. 5).<sup>27</sup> It is noteworthy that the exact pattern of **BBPQ-Ph** ( $R^1 = H$ ,  $R^2 = Ph$ ) could not be replicated with the benzodichalcogenophenes used in this work. To address this, the closest related examples for each chalcogen were employed for comparison, since quantum chemical calculations indicated that the choice of  $R^1$  and  $R^2$  does not affect the  $\pi$ -conjugated heptacyclic system (see Fig. 4 and the ESI for more details<sup>†</sup>). Substitution of the NH-group by sulfur, selenium or tellurium resulted in modified photophysical properties. Compound **9aa** showed blue-shifted absorption and emission maxima by 11–12 nm, leading to a similar Stokes shift of around  $2200\text{ cm}^{-1}$ , compared with **BBPQ-Ph**. Its optical gap of 3.38 eV was larger than that for **BBPQ-Ph** by 0.18 eV. A reverse trend was observed for selenium and tellurium substitutions. For **10aa**, the absorption and emission maxima were red-shifted by 15 nm and 55 nm, respectively, consequently reducing the optical gap by 0.1 eV, compared to **BBPQ-Ph**. This observation was even more significant for **11ba**, with absorption and emission maxima at 409 nm and 468 nm, respectively, resulting in a redshift of 45 nm and 73 nm and an optical gap of 2.88 eV, being 0.32 eV lower if compared to the NH-substituted counterpart. **BBPQ-Ph** exhibited the highest quantum yield among its counterparts, with 10%, compared to 1–4%. Despite structural discrepancies, the combination of enabling an ordered layered crystal packing motif through appropriate choice of  $R^1$  and  $R^2$ , along with choosing a chalcogen atom  $X$  as a substitute for NH, improves the potential for possible fabrication in organic devices, as discussed previously.

### Stability-measurements

Thermogravimetric analysis (TGA) and differential scanning calorimetry (DSC) were performed on **9bd**, **10bc** and **11ba**, each representing one distinct chalcogen within the BBCQs,

under a nitrogen atmosphere at a heating rate of  $10\text{ °C min}^{-1}$ . For the sulfur- and selenium-containing examples, no significant mass loss was observed at temperatures up to  $400\text{ °C}$  (for TGA & DSC-Plots see the ESI<sup>†</sup>). However, for the tellurium-doped sample, a slight mass loss of 5% was noted starting from  $366\text{ °C}$ . Overall, all three compounds exhibit a high thermal stability, enabling for potential vapor deposition onto device substrates.

## Conclusions

We present an efficient method for synthesizing chalcogen-substituted indolocarbazole-derivatives with a broad substrate scope of twenty-six examples. The isosteric replacement of the NH group with a chalcogen atom significantly influences the optical and theoretical band gaps. Moreover, we showed that while the introduction of peripheral substituents does not affect the band gap significantly, it does impact the structural properties. We extended the scope of previously reported benzobispyrrolo[3,2-*c*]quinolines (BBPQs) with the new class of benzobischalcogeno[3,2-*c*]quinolines BBCQs, allowing for more precise tailoring of electronic and structural properties in such heptacyclic conjugated  $\pi$ -systems. While oxygen nucleophiles can also be utilized to obtain benzofuran-moieties,<sup>42</sup> the synthesis of furan-substituted derivatives of BBCQs remains challenging. The reason lies in the presence of the *ortho*-aminoalkynyl units in our precursor molecules, favouring the formation of an indole when adding a strong oxygen-containing base, such as KOH. A high thermal stability was observed for some examples of the synthesized BBCQs, making these compounds promising candidates for incorporation into organic devices.

## Data availability

The authors declare that all the data used for this manuscript can be found in its ESI. The single crystal structures used in this manuscript have been assigned the CCDC 2380037–2380046.<sup>†</sup>





## Conflicts of interest

There are no conflicts to declare.

## Acknowledgements

C. H., J. K. and R. H. are grateful for the funding by the Deutsche Forschungsgemeinschaft (DFG; SFB 1249 – N-Heteropolyzyklen als Funktionsmaterialien). M. S. and A. S. K. H. are grateful for the funding by the Hector Fellow Academy. The authors acknowledge the support from the state of Baden-Württemberg through bwHPC and the German Research Foundation (DFG) through grant no INST 40/575-1 FUGG (JUSTUS 2 cluster). We thank Fabian Jester and Prof. Uwe Bunz (Heidelberg University) for TGA/DSC measurements.

## References

- M. L. Tomlinson, 177. Experiments on the preparation of indolocarbazoles. Part IV. The preparation of indolo[3': 2'-1: 2]carbazole, *J. Chem. Soc.*, 1951, 809–811.
- H. M. Grotta, C. J. Riggle and A. E. Bearnse, Preparation of Some Condensed Ring Carbazole Derivatives, *J. Org. Chem.*, 1961, **26**, 1509–1511.
- W. Lamm, W. Jugelt and F. Pragst, Photochemische Synthese von Carbazolen und Indolo[3, 2–b]carbazolen, *J. Prakt. Chem.*, 1975, **317**, 284–292.
- J. Tholander and J. Bergman, Syntheses of 6,12-disubstituted 5,11-dihydroindolo[3,2-b]carbazoles, including 5,11-dihydroindolo[3,2-b]carbazole-6,12-dicarbaldehyde, an extremely efficient ligand for the TCDD (Ah) receptor, *Tetrahedron*, 1999, **55**, 12577–12594.
- K. Kawaguchi, K. Nakano and K. Nozaki, Synthesis of ladder-type pi-conjugated heteroacenes via palladium-catalyzed double N-arylation and intramolecular O-arylation, *J. Org. Chem.*, 2007, **72**, 5119–5128.
- M. Vlasselaer and W. Dehaen, Synthesis of Linearly Fused Benzodipyrrole Based Organic Materials, *Molecules*, 2016, **21**, 785.
- A. S. K. Hashmi, Gold-catalyzed organic reactions, *Chem. Rev.*, 2007, **107**, 3180–3211.
- R. J. Harris and R. A. Widenhoefer, Gold carbenes, gold-stabilized carbocations, and cationic intermediates relevant to gold-catalysed enyne cycloaddition, *Chem. Soc. Rev.*, 2016, **45**, 4533–4551.
- A. S. K. Hashmi, Introduction: Gold Chemistry, *Chem. Rev.*, 2021, **121**, 8309–8310.
- C. M. Hendrich, K. Sekine, T. Koshikawa, K. Tanaka and A. S. K. Hashmi, Homogeneous and Heterogeneous Gold Catalysis for Materials Science, *Chem. Rev.*, 2021, **121**, 9113–9163.
- C. M. Hendrich, L. M. Bongartz, M. T. Hoffmann, U. Zschieschang, J. W. Borchert, D. Sauter, P. Krämer, F. Rominger, F. F. Mulks, M. Rudolph, A. Dreuw, H. Klauk and A. S. K. Hashmi, Gold Catalysis Meets Materials Science – A New Approach to  $\pi$ -Extended Indolocarbazoles, *Adv. Synth. Catal.*, 2021, **363**, 549–557.
- C. Wang, H. Dong, W. Hu, Y. Liu and D. Zhu, Semiconducting  $\pi$ -conjugated systems in field-effect transistors: a material odyssey of organic electronics, *Chem. Rev.*, 2012, **112**, 2208–2267.
- H. Shi, J. Dai, X. Wu, L. Shi, J. Yuan, L. Fang, Y. Miao, X. Du, H. Wang and C. Dong, A novel dimesitylboron-substituted indolo[3,2-b]carbazole derivative: Synthesis, electrochemical, photoluminescent and electroluminescent properties, *Org. Electron.*, 2013, **14**, 868–874.
- H.-C. Ting, Y.-M. Chen, H.-W. You, W.-Y. Hung, S.-H. Lin, A. Chaskar, S.-H. Chou, Y. Chi, R.-H. Liu and K.-T. Wong, Indolo[3,2-b]carbazole/benzimidazole hybrid bipolar host materials for highly efficient red, yellow, and green phosphorescent organic light emitting diodes, *J. Mater. Chem.*, 2012, **22**, 8399–8407.
- D. Chen, S.-J. Su and Y. Cao, Nitrogen heterocycle-containing materials for highly efficient phosphorescent OLEDs with low operating voltage, *J. Mater. Chem. C*, 2014, **2**, 9565–9578.
- K. Brunner, A. van Dijken, H. Börner, J. J. A. M. Bastiaansen, N. M. M. Kikken and B. M. W. Langeveld, Carbazole compounds as host materials for triplet emitters in organic light-emitting diodes: tuning the HOMO level without influencing the triplet energy in small molecules, *J. Am. Chem. Soc.*, 2004, **126**, 6035–6042.
- Z. Liang, Q. Tang, J. Xu and Q. Miao, Soluble and stable N-heteropentacenes with high field-effect mobility, *Adv. Mater.*, 2011, **23**, 1535–1539.
- Y. Li, Y. Wu, S. Gardner and B. S. Ong, Novel Peripherally Substituted Indolo[3,2– b ]carbazoles for High-Mobility Organic Thin-Film Transistors, *Adv. Mater.*, 2005, **17**, 849–853.
- A. Facchetti, Semiconductors for organic transistors, *Mater. Today*, 2007, **10**, 28–37.
- A. Mishra and P. Bäuerle, Small molecule organic semiconductors on the move: promises for future solar energy technology, *Angew. Chem., Int. Ed.*, 2012, **51**, 2020–2067.
- P. R. Nitha, S. Soman and J. John, Indole fused heterocycles as sensitizers in dye-sensitized solar cells: an overview, *Mater. Adv.*, 2021, **2**, 6136–6168.
- Q. Miao, T.-Q. Nguyen, T. Someya, G. B. Blanchet and C. Nuckolls, Synthesis, assembly, and thin film transistors of dihydrodiazapentacene: an isostructural motif for pentacene, *J. Am. Chem. Soc.*, 2003, **125**, 10284–10287.
- U. H. F. Bunz, N-heteroacenes, *Chem. – Eur. J.*, 2009, **15**, 6780–6789.
- T. Riehm, G. de Paoli, A. E. Konradsson, L. de Cola, H. Wadepohl and L. H. Gade, Tetraazaperopyrenes: a new class of multifunctional chromophores, *Chem. – Eur. J.*, 2007, **13**, 7317–7329.
- R. Heckershoff, T. Schnitzer, T. Diederich, L. Eberle, P. Krämer, F. Rominger, M. Rudolph and A. S. K. Hashmi,



- Efficient Synthesis of Dipyrrolobenzenes and Dipyrrolopyrazines via Bidirectional Gold Catalysis: a Combined Synthetic and Photophysical Study, *J. Am. Chem. Soc.*, 2022, **144**, 8306–8316.
- 26 J. Kahle, A. V. Mackenroth, C. Hüßler, P. D. Römgens, P. Schimanski, P. Krämer, M. Brückner, T. Oeser, F. Rominger, M. Rudolph and A. S. K. Hashmi, Modular synthetic strategies for dipyrrolopyrazines, *Org. Chem. Front.*, 2024, **11**, 2996–3003.
- 27 R. Heckershoff, L. Eberle, N. Richert, C. Delavier, M. Bruckschlegel, M. R. Schäfer, P. Krämer, F. Rominger, M. Rudolph and A. S. K. Hashmi, Versatile access to nitrogen-rich  $\pi$ -extended indolocarbazoles via a Pictet–Spengler approach, *Org. Chem. Front.*, 2022, **10**, 12–21.
- 28 W. Wu, Y. Liu and D. Zhu,  $\pi$ -conjugated molecules with fused rings for organic field-effect transistors: design, synthesis and applications, *Chem. Soc. Rev.*, 2010, **39**, 1489–1502.
- 29 S. Duhović and M. Dincă, Synthesis and Electrical Properties of Covalent Organic Frameworks with Heavy Chalcogens, *Chem. Mater.*, 2015, **27**, 5487–5490.
- 30 A. A. Jahnke and D. S. Seferos, Polytellurophenes, *Macromol. Rapid Commun.*, 2011, **32**, 943–951.
- 31 A. A. Jahnke, G. W. Howe and D. S. Seferos, Polytellurophenes with properties controlled by tellurium-coordination, *Angew. Chem., Int. Ed.*, 2010, **49**, 10140–10144.
- 32 P. Gao, D. Beckmann, H. N. Tsao, X. Feng, V. Enkelmann, W. Pisula and K. Müllen, Benzo[1,2-b:4,5-b']bis(benzothio)phene as solution processible organic semiconductor for field-effect transistors, *Chem. Commun.*, 2008, 1548–1550.
- 33 S. Guo, J. Wang, X. Fan, X. Zhang and D. Guo, Synthesis of pyrazolo[1,5-c]quinazoline derivatives through copper-catalyzed tandem reaction of 5-(2-bromoaryl)-1H-pyrazoles with carbonyl compounds and aqueous ammonia, *J. Org. Chem.*, 2013, **78**, 3262–3270.
- 34 S. Guo, L. Tao, W. Zhang, X. Zhang and X. Fan, Regioselective Synthesis of Indolo[1,2-c]quinazolines and 11H-Indolo[3,2-c]quinolines via Copper-Catalyzed Cascade Reactions of 2-(2-Bromoaryl)-1H-indoles with Aldehydes and Aqueous Ammonia, *J. Org. Chem.*, 2015, **80**, 10955–10964.
- 35 G. Abbiati, A. Arcadi, M. Chiarini, F. Marinelli, E. Pietropaolo and E. Rossi, An alternative one-pot gold-catalyzed approach to the assembly of 11H-indolo[3,2-c]quinolines, *Org. Biomol. Chem.*, 2012, **10**, 7801–7808.
- 36 A. Pictet and T. Spengler, Über die Bildung von Isochinolin-derivaten durch Einwirkung von Methylal auf Phenyl-äthylamin, Phenyl-alanin und Tyrosin, *Ber. Dtsch. Chem. Ges.*, 1911, **44**, 2030–2036.
- 37 E. D. Cox and J. M. Cook, The Pictet–Spengler condensation: a new direction for an old reaction, *Chem. Rev.*, 1995, **95**, 1797–1842.
- 38 S. Watanuki, K. Matsuura, Y. Tomura, M. Okada, T. Okazaki, M. Ohta and S.-I. Tsukamoto, Synthesis and pharmacological evaluation of 1-isopropyl-1,2,3,4-tetrahydroisoquinoline derivatives as novel antihypertensive agents, *Chem. Pharm. Bull.*, 2011, **59**, 1029–1037.
- 39 G. Tatsui, Über die Synthese von Carbolinderivaten, *J. Pharm. Soc. Jpn.*, 1928, **48**, 453–459.
- 40 A. S. Dillon and B. L. Flynn, Polyynes to Polycycles: Domino Reactions Forming Polyfused Chalcogenophenes, *Org. Lett.*, 2020, **22**, 2987–2990.
- 41 M. Nakano and K. Takimiya, Sodium Sulfide-Promoted Thiophene-Annulations: Powerful Tools for Elaborating Organic Semiconducting Materials, *Chem. Mater.*, 2017, **29**, 256–264.
- 42 R. Hudson, N. P. Bizier, K. N. Esdale and J. L. Katz, Synthesis of indoles, benzofurans, and related heterocycles via an acetylene-activated SNAr/intramolecular cyclization cascade sequence in water or DMSO, *Org. Biomol. Chem.*, 2015, **13**, 2273–2284.
- 43 R. J. Sundberg, in *Heterocyclic Scaffolds II*. ed. G. W. Gribble, Springer, Berlin, Heidelberg, 2010, pp. 47–115.
- 44 J. Seayad, A. M. Seayad and B. List, Catalytic asymmetric Pictet–Spengler reaction, *J. Am. Chem. Soc.*, 2006, **128**, 1086–1087.
- 45 D. S. McClure, Triplet-Singlet Transitions in Organic Molecules. Lifetime Measurements of the Triplet State, *J. Chem. Phys.*, 1949, **17**, 905–913.
- 46 F. Neese, Software update: The ORCA program system—Version 5.0, *Wiley Interdiscip. Rev.: Comput. Mol. Sci.*, 2022, **12**, e1606.
- 47 A. D. Becke, Density-functional thermochemistry. III. The role of exact exchange, *J. Chem. Phys.*, 1993, **98**, 5648–5652.
- 48 P. J. Stephens, F. J. Devlin, C. F. Chabalowski and M. J. Frisch, Ab Initio Calculation of Vibrational Absorption and Circular Dichroism Spectra Using Density Functional Force Fields, *J. Phys. Chem.*, 1994, **98**, 11623–11627.
- 49 F. Weigend and R. Ahlrichs, Balanced basis sets of split valence, triple zeta valence and quadruple zeta valence quality for H to Rn: Design and assessment of accuracy, *Phys. Chem. Chem. Phys.*, 2005, **7**, 3297–3305.
- 50 F. Weigend, Accurate Coulomb-fitting basis sets for H to Rn, *Phys. Chem. Chem. Phys.*, 2006, **8**, 1057–1065.

